

Prospects in innovative manufacturing technology of UHMWPE for prostheses and
comparison with medical grade UHMWPE

Ureczki Á., Keszei K.

Accepted for publication in Biomechanica Hungarica

Published in 2019

DOI: [10.17489/biohun/2019/1/04](https://doi.org/10.17489/biohun/2019/1/04)

PROSPECTS IN INNOVATIVE MANUFACTURING TECHNOLOGIES OF UHMWPE

Ágnes Ureczki, Kitti Keszei

Department of Polymer Engineering, Budapest University of Technology and Economics

ureczkia@pt.bme.hu

DOI: [10.17489/biohun/2019/1/04](https://doi.org/10.17489/biohun/2019/1/04)

Abstract

Due to its properties like high load-bearing capacity, biocompatibility, excellent abrasion resistance, and strength, ultra-high molecular weight polyethylene (UHMWPE) is widely used as a bearing material in industrial applications and in the field of joint prostheses. Currently, UHMWPE is produced by compression molding, ram extrusion, hot isostatic pressing and direct compression molding followed by post-processing techniques, such as milling or machining to finalize the prosthesis geometry and to achieve the final tolerances. With post-processing techniques, we are wasting a high-cost material, energy, and time. In this paper, we collected manufacturing technologies that have the potential to be used for creating parts with one-step production, minimalized material loss, and with a view of providing customized manufacturing capabilities. We compared two technologies: (i) FFF printing and (ii) injection-molding. In addition to the feasibility, we focus on the investigation of mechanical properties. Three tests were performed on the manufactured specimens: hardness measurement, tensile test, and scanning electron microscope (SEM).

Keywords: UHMWPE; prosthetics; injection molding; 3D printing; FFF

Introduction

Owing to its high load-bearing capacity, biocompatibility, outstanding mechanical properties, and excellent abrasion resistance, ultra-high molecular weight polyethylene (UHMWPE) is widely used in the industry and also in medical fields, such as in joint prostheses.¹

Manufacturing technologies for producing UHMWPE are compression molding, ram extrusion, hot isostatic pressing, and direct compression molding.¹ They use powder resin produced from ethylene gas by polymerization with the use of the Ziegler process.² Recently we can also find granules form of the

UHMWPE on the market, recommended for injection molding, but it is still hard to process the material as it requires high pressure.¹ Its extremely low melt flow rate (MFR = 0.06 g/10 min) and high melt viscosity make the material difficult to process even in the melting state.¹ Although, most of the powder resin-based manufacturing technologies require post-processing techniques, such as milling to finalize the geometry and to achieve the final tolerances.¹ With these post-processing operations, we are wasting material, energy, and time. This is one of the reasons it is important to turn to alternative techniques. We focused on the FFF technology (Fused Filament Fabrication), a layer-by-layer extrusion technique, and injection molding. FFF

technology is recommended for parts in low volumes and parts with unique, customized complex geometries. In the medical field, such as in temporomandibular joint replacement and total knee joint replacement³⁻⁵ the technique could be a beneficial technology from the production side. In the case of standard-sized parts with medium or high volumes, examining injection molding is recommended, which can be used to create complex geometries cost-effectively and fast. In both technologies, we can build the parts from granule form and create products with material addition.

We aim to explore the FFF processability of the material. Based on a literature review, there are different ways of improvements in the field of additive manufacturing. One is working with the SLS⁶ technology, using the powder form of the material, and others working with the FFF^{7,8} technology, using the filament form of the material. Although there was no precedent for FFF printing pure UHMWPE successfully due to its difficulties in processing, the possibility of additive usage allows us to optimize processing parameters and product attribute parameters, hence to make the processing technology viable. Panin et al.⁹ optimized the plasticizing components ratio of the UHMWPE matrix for keeping its excellent mechanical properties but making it easier to produce by the FFF technology (UHMWPE + 15 wt. % HDPE-g-SMA + 15 wt. % PP). With this material, they could even achieve much better tribological properties (1, 4 times) on the 3D printed parts than on the parts produced from the same material by hot-pressed technology. Based on their studies, they recommend fabricating the material by FFF printing for tribomechanical purposes. In the field of injection molding of the UHMWPE material, we can see that it is challenging to process. Some of the analyzed literatures deal with the elimination of the delamination

layers derived from the processing technology,¹⁰ while others deal with the development of the manufacturing technology or additives to make the raw material easier to process.¹¹ Some researches¹² examine the tribological behavior of injection molded UHMWPE.

In this paper, we examined the novel manufacturing technologies of the material, which can be used for creating beneficial products in the long run. We aim to compare two technologies: FFF technology and injection-molding. In addition to the feasibility, we focus on the investigation of the mechanical properties. Our future perspective is to optimize the technology for the UHMWPE material and check the effects of its mechanical, tribological, and morphological properties. Our first step, presented in this paper, is the examination of the feasibility and the mechanical properties of specimens fabricated by the FFF technology.

Materials and methods

During the preliminary experiments, the L4000 (Lubmer, Mitsui Chemicals) commercial-grade UHMWPE was used. The filament for FFF printing was created by a twin-screw extruder, FFF printing was done on a CraftBot3, dual head FFF printer. The machine settings for sample preparation have been optimized manually and will be detailed in a later section. The injection-molded specimens were fabricated by an Arburg 420 C injection molding machine. Three tests were performed on the manufactured specimens: hardness measurement, tensile test, and scanning electron microscope (SEM). Plates were injection molded first then the specimens were milled out of them. A Roland MDX-540 milling machine was used for milling. We used EN ISO 527 5A test specimens for the examinations. Shore D hardness was determined with a Zwick 3114. The tensile tests were performed on a Zwick Z005

Parameter	Value
Injection temperature of the zones [°C]	225-230-235-240-240
Mold temperature [°C]	40
Holding pressure [MPa]	70
Time for holding pressure [s]	20
Injection rate [cm ³ /s]	40

Table 1. Injection molding parameters

universal tensile testing machine. The SEM investigations were performed with a Jeol JSM 6380LA scanning electron microscope.

The injection molding settings were determined, taking into account the recommendations on the raw material datasheet. 80x80x4 mm plates with film gates were injection molded using a two-cavity mold. The test specimens were obtained by

milling from the injection molded plates. The milling velocity was 12 mm/s, and the speed was 3000 1/min.

Our experiment focused on finding an FFF parameter configuration that can be used to produce specimens from UHMWPE. The biggest challenge during processing the material was to keep the first layer of the material on the bed. From the originally used kapton film coated bed the material started to shrink out immediately. Therefore, we tried different techniques to ensure the good adhesion. A positive result was obtained with a perforated plate. Table 2 summarizes the process of keeping the first layers attached to the printing bed. The main problem was the high shrinkage of the material.

Table 3 shows the constant and changed parameters used during the process. We worked with high temperature, high infill densities and




Type of bed	Efficiency	Comment/Illustration
Glass with kapton film	No adhesion	No layers remained on the plate.
Atactic PP liquid (Vestoplast W-1750)	The first layer adhered successfully, but the material came up when additional layers were printed.	
Epoxy-based printed circuit board perforated plate	Feasible. It warmed up but did not soften under the applied temperatures.	
UHMWPE injection molded plate	Proper adhesion, but removal is not feasible from the plate. Furthermore, the plate melted and the extruder head moved on it.	

Table 2. Bed types and their efficiency for keeping the layers on the bed

	Parameter	Value	Optimal value
Constant	Extrusion temperature [C°]	300	-
	Bed temperature [C°]	110	-
	Layer height [mm]	0,2	-
	Infill structure	parallel lines (-45°/45°)	-
	Infill density [%]	100	-
Changed	Number of rafts	0-2-5	2
	Infill density of the raft layers [%]	10-50-60-70-80-90-100	100
	Extruded material [%]	100-110	110
	Extrusion speed [mm/s]	10-20	10
	Printing orientation	flat / on-edge	flat
	Use of a dome and door	yes-no	yes

Table 3. FFF printing parameters setup

low printing speed to ensure adequate heating of the material. We also used a dome and a door from Craftbot spare parts to achieve an increased temperature of the environment.

The heating and cooling cycles affect the material behaviour and the non-uniform thermal gradients evacuation. Consequently, thermal stresses can accumulate within the part, which can affect the dimensional accuracy and quality (e.g. distortion, warpage) of the printed structure. Thanks to the heated bed, the temperature of the lower layers is higher and the effect of the heated bed during the process is less and less pronounced.¹³

To maximize the physical connection between the specimen and the perforated sheet, we first

printed a “raft” under the specimen. This is a larger tray of material printed in few layers before the actual print. In the experiments, printability worked if this “raft” did not consist of more than two layers. *Figure 1* shows the mentioned raft, and also shows that in case of more than two layers of the raft, the material started to shrink out from the perforated plate.

It was advisable to wait until the whole specimen cooled down, otherwise, the printed product would have a greater deformation after the removal from the perforated plate. From the printed parts, we firstly removed the raft layer. It is important to consider that it was impossible to print thin parts, and also, it was also impossible to print complex geometries. *Figure 2* shows that we can only print samples with flat print-



Figure 1. Raft layer evaluation during the process

ing orientation. Although the edges of the specimens are inaccurate in this case, too. The cross-section dimensions are well reproducible, so it can be used for the performed tests.

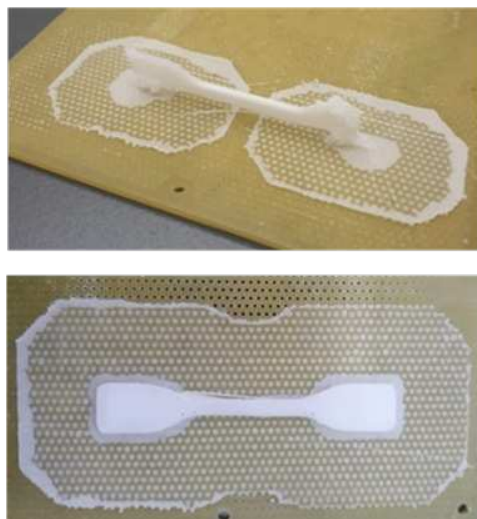


Figure 2. Printed specimens with different orientations

Results

The hardness measurement results show that the fibrous structure of the FFF printed sample influences its hardness. We measured on a surface that appeared to be homogeneously compact. The measured values are given in Table 4. Lower shore D value measured on the printed samples. It could be caused by its layer by layer structure. We also measured a higher standard deviation value on the FFF printed samples. The injection-molded samples were more homogenous, all 5 measurements have the same hardness value.

The main parameters used in the tensile test are the following: the clamping distance was 50 mm, the preload was 1 N with 10 mm/min preload speed. The temperature during the measurement was 23.3 °C and the relative humidity was 26.8%. We examined 5-5 specimens of each manufacturing technology and plotted the stress-strain curves of each and their average (Figure 3). Table 5 shows the characteristic values that can be calculated from the tensile measurement. The curves show different trajectories. The calculated modulus and strength values were lower in the case of the FFF printed than the injection-molded specimens. The different behaviour of the samples can be explained by the orientation of the UHMWPE chains, which is greatly influenced by firstly both filament production and FFF printing and secondly by injection-molding. Elongation at tensile strength is higher in the case of the FFF printed specimens, but elongation at break is significantly lower. It is also important to highlight that there are significant standard deviations mainly in elongation at break in injection-molded parts, which could show that with milling, we probably caused minor surface mistakes on the samples.

During scanning electron microscopy (SEM), we worked at 30-, 100- and 200-fold magnifications. The study aimed to compare the morphological structure of the injection-molded and FFF printed specimens and to investigate the failure characteristics of the FFF printed sample. An accelerating voltage of 10 kV was used. Figure 4 shows the separation

Sample type	Specimen	Shore D average hardness	Standard deviation
A	L4000, injection molded	63,85	0,34
B	L4000, FFF printed	57,20	0,86

Table 4. Shore D average harnesses

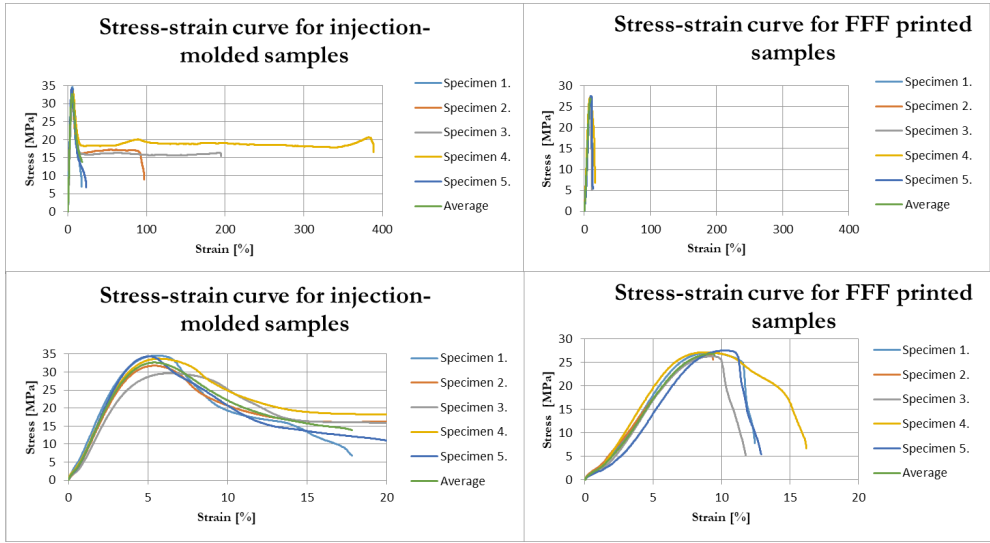


Figure 3. Stress-strain curves

of the first layer from the printed raft in the FFF printed sample, highlighted the air gap between the raft and the first layers. Figure 5 shows an (I) injection-molded sample broken in liquid nitrogen, (II) an FFF printed sample broken in liquid nitrogen, and (III) an FFF printed sample after the tensile test at 30x 200x magnifications. If we focus on the central areas of the FFF printed pattern (and not on the bottom, base layer), we do not see significant differences. The tensile test results show higher

elongation at break in the case of the injection-molded samples. This high elongation could be explained by the formed “skin-core-skin” structure. Because the injection-molded plates are relatively thick, the core structure dominates in their case, where the orientation of the molecules is less significant. In contrast, in the case of the FFF technology, the fibers are highly oriented. This could be one of the reasons for the different elongation behavior of the samples produced by different technologies.

Property	Injection-molding	standard deviation	FFF printing	standard deviation
Tensile strength: σ_M [MPa]	32,80	1,703	26,92	0,405
Elongation at tensile strength: ϵ_M [%]	5,64	0,426	9,29	0,447
Ultimate tensile strength: σ_R [MPa]	10,95	3,854	10,17	7,092
Elongation at break: ϵ_R [%]	144,56	126,000	12,54	7,092
Young's modulus: E_h [GPa]	0,68	0,043	0,39	0,045

Table 5. Calculated values from tensile test



Fig. 4. FFF printed UHMWPE first layer at 100x magnification

It can be also clearly seen from the figure that although the FFF printed samples obtained from the tensile test showed a small elongation at break, the failure of the material is not brittle. For a deeper understanding of the mechanical and morphological properties of the material, further experiments and studies are required.

Discussion

In our research, we investigated the FFF

printability of UHMWPE. During our study, we explored the validity of the topic. The favorable mechanical properties of the material and the successful and widely spread use in healthcare, causing the importance of examining new processing technologies. With FFF technology, as the novel method, we can create customized unique geometries. This is one of the reasons why this technology has great importance. In our research, we examined whether it is possible to process the pure UHMWPE material with FFF technology because of the mentioned advantages. During the experiments, it was possible to produce limited specimens made of pure UHMWPE by optimizing the process parameters and using a perforated plate to make physical contact between the UHMWPE layers and the plate.

Still, it was not possible to create complex geometries. Beyond the high processing temperatures, the challenge was the high shrinkage of the material and to ensure good adhesion between the first and base plate layers. The hardness of the test specimens was compared to the samples of the same material

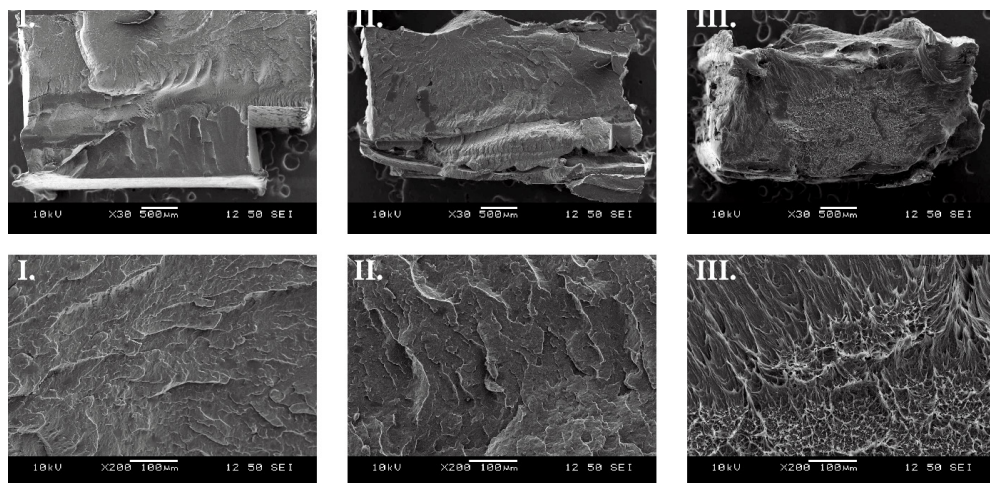


Fig. 5. Injection-molded cryogenic (I.), FFF printed cryogenic (II.) and FFF printed surfaces after tensile test (III.) at 30x and 200x magnifications

made by injection-molding, then tensile test and electron microscopic examination were performed. The FFF printed products showed inferior hardness, lower strength, and modulus than the injection-molded samples. SEM pictures show that the first layer adhesion is a critical part. The filament extrusion and also the FFF printing itself affects the properties of the material and the orientation of the

molecular chains. It is important for further examinations to find out how we can minimize shrinkage and create complex products with appropriate dimensional accuracy. Moreover, further measurements are required to verify if the changed material structure and properties are still between favorable limits to allow the usage of FFF printed part in different applications.

REFERENCES

1. Kurtz SM, editor. UHMWPE Biomaterials Handbook. 3rd ed. Amsterdam, The Netherlands: Elsevier Inc.; 2016.
2. Padmanabhan S, Sarma KR, Sharma S. Synthesis of ultrahigh molecular weight polyethylene using traditional heterogeneous Ziegler-Natta catalyst systems. *Industrial & Engineering Chemistry Research* 2009;48(10): 4866-4871.
3. Ackland DC, Robinson D, Redhead M, Lee PVS, Moskaljuk A, Dimitroulis G. A personalized 3D-printed prosthetic joint replacement for the human temporomandibular joint: From implant design to implantation. *Journal of the Mechanical Behaviour of Biomedical Materials* 2017;69: 404-411.
4. De Meurechy N, Braem A, Mommaerts MY. Biomaterials in temporomandibular joint replacement: current status and future perspectives - a narrative review. *International Journal of Oral and Maxillofacial Surgery* 2017;47(4): 518-533.
5. Szojka A, Lalh K, Andrews SHJ, Jomha NM, Osswald M, Adesida AB. Biomimetic 3D printed scaffolds for meniscus tissue engineering. *Bio-printing* 2017;8: 1-7.
6. Rimell JT, Marquis PM. Selective laser sintering of ultra high molecular weight polyethylene for clinical applications. *Journal of Biomedical Materials Research* 2000;53(4): 414-420.
7. Bin Md Ansari MH, Irwan Bin Ibrahim MH. Thermal characteristic of waste-derived hydroxyapatite (HA) reinforced ultra high molecular weight polyethylene (UHMWPE) composites for fused deposition modelling (FDM) process. *Proceeding of Colloquium of Advanced Mechanincs (CAMS2016)*; 2016 Dec 18-19; Johor, Malaysia. IOP Conference Series: Materials Science and Engineering; 2017.
8. Panin SV, Buslovich DG, Kornienko LA, Alexenkov VO, Dontsov YuV, Shil'ko SV. Structure, as well as the tribological and mechanical properties, of extrudable polymer-polymeric UHMWPE composites for 3D printing. *Journal of friction and wear* 2019;40(2): 143-153.
9. Panin SV, Buslovich DG, Kornienko LA, Alexenkov VO, Dontsov YuV, Ovechkin BB. Structure and tribomechanical properties of extrudable ultra-high molecular weight polyethylene composites fabricated by 3D printing. *Proceedings of Oil and Gas Engineering Conference*; 2019 Feb 26-28; Omsk, Russian Federation. AIP Conference Proceedings; 2019.
10. Yilmaz G, Yang H, Turng L. Injection molding of delamination-free ultra-high-molecular-weight polyethylene. *Polymer Engineering & Science* 2019;59(11): 1-10.
11. Xie M, Chen J, Li H. Morphology and mechanical properties of injection-molded ultrahigh molecular weight polyethylene/polypropylene blends and comparison with compression molding. *Journal of Applied Polymer Science* 2019;111: 890-898.
12. Raffi NM, Kanagarajan D, Srinivasan V. Tribo-

logical behaviour of ultra-high molecular weight polyethylene in a hip joint simulator. *Frontiers of Material Science* 2012;6(4): 358–365.

13. Kousiatza C, Chatzidai N, Karalekas D. Temperature mapping of 3D printed polymer plates: Experimental and numerical study. *Sensors* 2017;17(3): 456.

Hereby we would like to thank our supervisor Dr. Norbert Krisztián Kovács and my consultant Dr. Gábor Szabényi, who supported the preparation of this paper with the best of their professional knowledge. We would also like to thank the Laboratory Staff of the Department of Polymer Engineering, but especially to Dávid Bartók, György Bartók and István Horváth for their help in preparing the measurements.

The research reported in this paper and carried out at BME was supported by the NRDI Fund (TKP2020 IES, Grant No. BME-IE-BIO) based on the charter of bolster issued by the NRDI Office under the auspices of the Ministry for Innovation and Technology.

The project is funded by the National Research, Development and Innovation (NKFIH) Fund, Project title: „Developing a new generation of customized medical implants and medical aids for additive technologies”; the application ID number: NVKP_16-1-2016-0022. Lubmer L4000 material was supported by Dreyplas GmbH.

Ágnes Ureczki

Budapest University of Technology and Economics, Faculty of Mechanical Engineering,
Department of Polymer Engineering

Műegyetem rkp. 3., T. bldg. III., Budapest, Hungary, H-1111

Tel.: (+36) 1 463-3083

Pannon

csípőprotézis szár család

Világszínvonal,
egyetlen műszerkészlettel!

